Semiclassical accuracy in phase space for regular and chaotic dynamics

L. Kaplan
Department of Physics, Tulane University, New Orleans, Louisiana 70118, USA
(Received 21 April 2004; published 31 August 2004)

A phase-space semiclassical approximation valid to $O(\hbar)$ at short times is used to compare semiclassical accuracy for long-time and stationary observables in chaotic, stable, and mixed systems. Given the same level of semiclassical accuracy for the short time behavior, the squared semiclassical error in the chaotic system grows linearly in time, in contrast with quadratic growth in the classically stable system. In the chaotic system, the relative squared error at the Heisenberg time scales linearly with $\hbar_{\mathrm{eff}}$, allowing for unambiguous semiclassical determination of the eigenvalues and wave functions in the high-energy limit, while in the stable case the eigenvalue error always remains of the order of a mean level spacing. For a mixed classical phase space, eigenvalues associated with the chaotic sea can be semiclassically computed with greater accuracy than the ones associated with stable islands.

DOI: 10.1103/PhysRevE.70.026223 PACS number(s): 05.45.Mt, 03.65.Sq

I. INTRODUCTION

Semiclassical methods have a long history traceable to the very beginnings of the "old quantum theory" and serve two interrelated purposes in many areas of physics. First, semiclassical methods provide valuable approximation techniques in situations where a full quantum calculation is either impossible or unnecessary. Equally importantly, semiclassical methods provide a link between quantum results and our classical intuition, and allow us to separate physical behavior that is due simply to classical paths and their interference from behavior that is attributable to nonclassical processes such as tunneling or diffraction.

For strongly chaotic systems, purely *classical* calculations in d dimensions that ignore phase effects must break down at the mixing time or log time $T_{\log} \sim \lambda^{-1} \ln N \sim \lambda^{-1}(d-1)\ln \hbar_{\mathrm{eff}}^{-1}$, where λ is the maximal Lyapunov exponent of the classical dynamics and $N \sim \hbar_{\mathrm{eff}}^{-(d-1)}$ is the effective dimension of the accessible Hilbert space, or the size of the accessible classical phase space in Planck cell units. This breakdown of *classical*-quantum correspondence occurs because beyond the mixing time, multiple classical paths connect a generic initial state to a generic final state, and interference effects become $O(1)$. On the other hand, in a series of papers, Heller and co-workers showed that *semiclassical* calculations in chaotic systems, which include the effect of interference between distinct classical paths, can follow the quantum propagator at times well beyond the mixing time [1]. An estimate for the breakdown time scale of semiclassical-quantum correspondence was obtained by quantifying the effects of caustics for a stadium billiard [2].

Over the past decade, significant light has been shed on the issue of semiclassical accuracy and its breakdown in diverse chaotic and regular systems. For example, Boasman has used a semiclassical approximation to the boundary integral method to obtain a semiclassical spectrum for two-dimensional chaotic billiards, observing an overall semiclassical spectral shift as compared with the exact quantum spectrum, in addition to small random fluctuations [3]. On the other hand, Prosen and Robnik have shown the complete failure of torus quantization to reproduce the spectra of two-dimensional *integrable* billiards, such as the circle billiard [4], suggesting that integrability may in some cases lead to an increase of semiclassical errors; Rahav *et al.* have obtained more recent results consistent with this conclusion [5]. Primack and Smilansky were among the first to analyze semiclassical accuracy for three-dimensional chaotic systems, focusing on including corrections to the state-counting function beyond the leading Weyl term [6].

Main and collaborators have developed the powerful harmonic inversion technique for accurate and efficient semiclassical calculations of energies, resonances, and matrix elements [7]. This technique, as well as the earlier cycle-expansion method [8] were applied recently to the four-sphere scattering problem, demonstrating a high degree of accuracy at a greatly reduced computational cost compared with brute-force quantum calculations [9]. Another promising recent approach, put forward by Vergini and co-workers, involves the accurate construction of quantum eigenstates as linear superpositions of "scar functions" associated with short unstable periodic orbits [10].

In the time domain, statistical arguments concerning the propagation of semiclassical errors have shown that semiclassical error in chaotic systems accumulates incoherently, and thus the squared error typically grows only linearly with time, in contrast with quadratic growth for the regular case [11]. Transforming to the energy domain, this implies that semiclassical methods are generically more accurate for computing wave functions and eigenvalues for chaotic systems than for regular ones, in the $\hbar_{\mathrm{eff}} \to 0$ (or high energy) limit. In particular, for $d=2$, analytical arguments and numerical tests show that eigenvalues can be semiclassically resolved with great accuracy for chaotic systems, for sufficiently small $\hbar_{\mathrm{eff}}$, while in the regular case even the order of eigenvalues cannot be unambiguously determined semiclassically. This result has been related to the reduction of the quantization ambiguity in chaotic systems [12] and to the slower decay of fidelity in the presence of strong chaos (as long as the perturbation has nonzero diagonal matrix elements in the basis of the unperturbed system) [13].

Both the theoretical analysis and the numerical tests in Ref. [11] were performed for semiclassical evolution in the position representation, i.e., for the Van Vleck–Gutzwiller propagator [14]. Although well suited for the model systems treated in that work, position-representation semiclassics suffers in general from the problem of proliferation of caustics, which eventually dominate the semiclassical propagator [2]. The problem becomes particularly acute when one attempts to compare semiclassical dynamics in hard chaotic systems with that in a regular system or in a mixed phase space. Semiclassical calculations in a phase space basis are more natural from the point of view of classical-quantum correspondence and have the inherent advantage of allowing direct comparison between time evolution in chaotic, regular, and mixed systems, without the result being overwhelmed by the problem of position-space or momentum-space caustics.

The aim of this paper is to improve our understanding of semiclassical accuracy in a phase space representation, as a function of time and $\hbar_{\text{eff}}$, and to directly compare the behavior of the semiclassical error in chaotic, regular, and mixed systems. The organization is as follows. In Sec. II we briefly present the model and the method used for performing semiclassical and quantum calculations in phase space. Theoretical expressions for semiclassical accuracy in chaotic systems are presented in Sec. III A, along with supporting numerical data from the model system. In addition to generalizing the analysis of Ref. [11] from position space to a phase space representation, we explicitly test the prediction of Ref. [11] concerning the linear growth with the time of the mean squared semiclassical error, as well as the prediction of linear decrease with $\hbar$ of the error at the Heisenberg time. This is followed by a similar analysis for regular and mixed systems, in Secs. III B and III C, respectively. Finally, Sec. IV summarizes the results and presents an outlook for the future.

II. MODEL AND METHOD

Although our theoretical analysis applies quite generally to two-dimensional noninteracting systems, we simplify the numerical simulations by focusing on one-dimensional kicked maps, which share most scaling and other physical properties of this class of systems [15]. The discrete-time map can be regarded as a Poincaré surface of section of a two-dimensional system with Hamiltonian dynamics. Specifically, we parametrize the one-step map on a toroidal classical phase space $(q,p) \in [0,1) \times [0,1)$ as

$$p_0 \to p_1 = p_0 - V'(q_0) \bmod 1,$$

$$q_0 \to q_1 = q_0 + T'(p_1) \bmod 1, \tag{1}$$

where

$$V(q) = -\frac{1}{2} m_q q^2 - \frac{K_q}{(2\pi)^2} \sin(2\pi q),$$

$$T(p) = \frac{1}{2} m_p p^2 + \frac{K_p}{(2\pi)^2} \sin(2\pi p). \tag{2}$$

The dynamics is iterated to obtain classical evolution over many kicks (or many bounces in the corresponding two-dimensional Hamiltonian system). For values $m_q = m_p = 1$ and $0 < |K_q|, |K_p| < 1$, for example, we obtain the purely chaotic perturbed cat map, or kicked inverted oscillator, while for $m_q = -1$, $m_p = 1$ and small K_q, K_p, the dynamics is predominantly regular, corresponding to a kicked regular oscillator. Parameters K_q and K_p are essential to introduce nonlinearity into the dynamics (if $K_q = K_p = 0$, the semiclassical propagator is exact, for any integers m_q and m_p). The above four parameters can also be adjusted to vary the Lyapunov exponent in the chaotic regime, or to study a mixed phase space, as we will see below in Sec. III.

The one-step quantum evolution matrix for the above system takes the very simple form

$$\hat{U}_1 = \exp[-i\hat{T}(\hat{p})/\hbar]\exp[-i\hat{V}(\hat{q})/\hbar], \tag{3}$$

which again may be iterated or diagonalized to obtain long-time or stationary behavior, $\hat{U}_t = [\hat{U}_1]^t$. As discussed in the introduction, we will apply this propagator to Gaussian wave packets (or coherent states) centered at phase space points (q_k, p_k):

$$\phi_k(q) = \mathcal{N} \exp[-(q-q_k)^2/2\hbar + ip_k(q-q_k)/\hbar], \tag{4}$$

where N is a normalization constant.

Unfortunately, there is not a unique and universally used semiclassical approximation for wave packet evolution, analogous to the Van Vleck–Gutzwiller expression in position or momentum space. Several methods have been proposed that differ in both the order (in $\hbar_{\text{eff}}$) of the semiclassical error at fixed time t and in the numerical size of that error. The so-called "thawed Gaussian" approximation, for example, allows the shape of the Gaussian wave packet to change as it evolves under a locally quadratic potential $V(q)$ [16]. An alternative approach uses "frozen" or unspreading wave packets [17]. Another coherent state method retains the stationary phase idea of the Van Vleck–Gutzwiller propagator but extends dynamics into complex phase space [18]. It is possible instead to work in complex time while retaining real initial conditions in phase space [19].

In the present work, we are not interested in reducing the numerical size of the semiclassical error but only in understanding its scaling properties with t and $\hbar_{\text{eff}}$, for regular and chaotic systems. For this reason, we will choose what is a convenient method for our purposes, noting that the results would hold for any semiclassical approximation valid to the same order in $\hbar_{\text{eff}}$. We essentially use a variation of the thawed Gaussian method, extended to next-to-leading order in $\sqrt{\hbar_{\text{eff}}}$, and then calculate semiclassically the overlaps of the time-evolved "thawed" Gaussians with the Gaussians in the original basis [20].

Specifically, we start with a (nonorthogonal) complete set of $N = 1/2\pi\hbar$ Gaussians ϕ_j of the form given in Eq. (4), with the center points (q_j, p_j) offset slightly from a rectangular

grid to reduce numerical instabilities. The semiclassical overlap matrix

$$A_0(j,k) = \langle \phi_j | \phi_k \rangle_{\mathrm{SC}} \tag{5}$$

is obtained analytically by Gaussian integration. To evaluate the t-step semiclassical propagator $A_t(j,k)$ between initial Gaussian ϕ_k and final Gaussian ϕ_j, we find real classical trajectories from (q_0,p_0) to (q_t,p_t) in time t that minimize $(q_0-q_k)^2+(p_0-p_k)^2+(q_t-q_j)^2+(p_t-p_j)^2$, i.e., all trajectories that start near the center of Gaussian k and end near the center of Gaussian j after t steps. Of course for fixed t and sufficiently small $\hbar$ $(t<T_{\log}\sim\lambda^{-1}\ln\hbar^{-1})$, there will be at most one such trajectory, and in principle that is all we need even for our long-time analysis, as will be seen below. In practice, however, for finite values of $\hbar$ we include all contributing trajectories. For each trajectory, the potential $V(q)$ is expanded to *third* order around the starting position of the trajectory, q_0. When this potential is applied to the original Gaussian ϕ_k, we obtain a wave packet of the form

$$\begin{aligned}&\exp[a + b(q-q_0) + c(q-q_0)^2 + d(q-q_0)^3] \\ &= \exp[a + b(q-q_0) + c(q-q_0)^2] \\ &\quad\times[1 + d(q-q_0)^3 + O(\hbar)],\end{aligned} \tag{6}$$

where a, b, c, and d are complex numbers of order $\hbar^{-1}$, and therefore $q-q_0$ is $O(\hbar^{1/2})$. We note that an "extended" semiclassical dynamics [21], which truncates the expansion of the Hamiltonian at third order rather than second order is needed to keep the error in the one-step phase space propagator at $O(\hbar)$, consistent with the error in the Van Vleck–Gutzwiller propagator in position space [14].

The wave packet of Eq. (6) may now be rewritten, via Fourier transform, as a momentum space wave packet having the same form but expanded in powers of $p-p_1$ instead of $q-q_0$. The kinetic term $T(p)$ of the Hamiltonian may now be applied, again expanded to third order in $p-p_1$. Then, the packet is Fourier transformed back to position space and the procedure is repeated t times. At the end of t steps, we may analytically find the overlap between the semiclassically evolved t-step wave packet $\phi_{k,\mathrm{SC}}(t)$, still having the form of Eq. (6), and the final Gaussian wave packet ϕ_j to obtain the semiclassical propagator $A_t(j,k)$. If several classical paths lead from the vicinity of ϕ_k to the vicinity of ϕ_j in time t, their contributions must be summed to produce the semiclassical amplitude $A_t(j,k)$, just as in the Gutzwiller expression. As we will see in Sec. III A, for a chaotic system the long-time semiclassical propagator may be arbitrarily well approximated (in the $\hbar\to 0$ limit) using only the matrix A_t for $1\ll t\ll T_{\log}$, where at most one path contributes to each matrix element. However, as we are dealing with finite $\hbar$ in our numerical simulations, we will always use the sum over all classical paths in numerical calculations.

III. SEMICLASSICAL ACCURACY

A. Chaotic dynamics

As discussed previously in the context of position-space semiclassical propagation, direct comparison between quantum and semiclassical evolution at long times for a chaotic system, or between quantum and semiclassical stationary properties for such a system, faces the obstacle of the exponential proliferation of classical paths [1]; an analogous problem of exponential growth in the number of periodic orbits exists in the energy domain [14,8,23]. This proliferation seemingly makes long-time semiclassical propagation in a classically chaotic system an exponentially harder problem than the full quantum evolution, puts into question the convergence of long-time semiclassical dynamics to any stationary behavior, and prevents the comparison of semiclassical and quantum stationary properties for small $\hbar$. The threefold difficulty can be addressed using the idea that the Heisenberg uncertainty principle washes out information on scales below $\hbar$, and thus the total amount of semiclassical information is finite for all times and scales only as a power of $\hbar$. We can therefore collect, consolidate, and iterate semiclassical amplitude on sub-$\hbar$ scales, obtaining the full semiclassical long-time dynamics to arbitrary accuracy in polynomial computation time. This "semiclassical path consolidation" idea has previously been used successfully to investigate long-time semiclassical accuracy in the position representation for chaotic dynamics [20,11] and to demonstrate the semiclassical nature of dynamical localization in one dimension [22]. Conceptually, the approach is similar to cycle expansion methods in periodic orbit theory [8,23]; however, no information about periodic orbits is needed here. Instead of accounting for long-time semiclassical behavior in terms of periodic paths up to period $\tau_{\mathrm{periodic}}\sim T_{\log}$, we use *all* short paths up to length $\tau\sim 1$. In the following, we adapt the methods of Ref. [11] to a phase space representation, and refer the reader to that earlier paper for a detailed discussion.

We begin by noting that although semiclassical dynamics is not multiplicative, due to the fact that a concatenation of two stationary paths is in general not stationary, we may nevertheless write

$$\begin{aligned}A_{t_1+t_2}(j,k) &= \sum_{\ell,\ell'} A_{t_2}(j,\ell')A_0^{-1}(\ell',\ell)A_{t_1}(\ell,k) + O(\hbar) \\ &= [A_{t_2}A_0^{-1}A_{t_1}](j,k) + O(\hbar),\end{aligned} \tag{7}$$

where the $O(\hbar)$ error is due to the intermediate sums being done exactly rather than by stationary phase, and the inverse of the semiclassical overlap matrix A_0 is necessary due to nonorthogonality. In general, we may approximate the true time-t semiclassical propagator A_t by evaluating the exact semiclassical dynamics to some "quantization time" τ and then iterating the resulting matrix:

$$A_{t,\tau} = A_{t \bmod \tau}[A_0^{-1}A_\tau]^{[t/\tau]}, \tag{8}$$

where $[t/\tau]$ is the integer part of t/τ. We may call $A_{t,\tau}$ the "τ-semiclassical" propagator. For $\tau=1$, $A_{t,\tau}$ is the one-bounce semiclassical quantization pioneered by Bogomolny [24]. For a continuous-time system, the $\tau\ll 1$ limit is equivalent to quantum propagation via the Feynman path integral approach. The exact time-t semiclassical propagator, on the other hand, is recovered in the opposite limit when the quantization time approaches t:

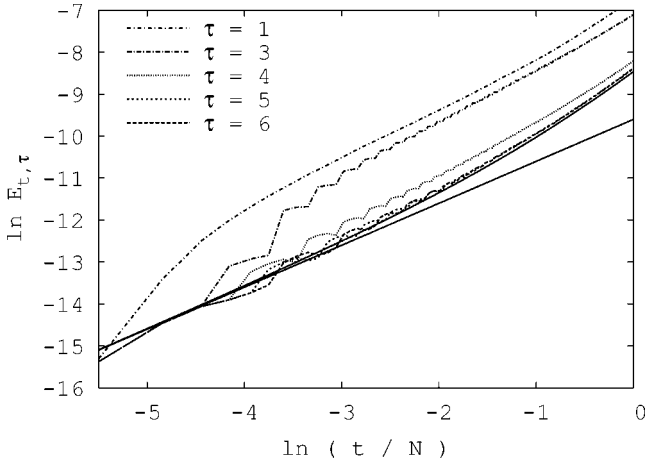

FIG. 1. The mean squared τ-semiclassical error $E_{t,\tau}$ in a chaotic system is plotted as a function of t/N for semiclassical parameter $N=256$ and for several values of the quantization time τ. For $\tau \gg 1$, $E_{t,\tau}$ is a reliable proxy for the true semiclassical error E_t. The classical system parameters for Eq. (2) are $m_q=m_p=1$; $K_q=K_p=1/2$. The lower and upper solid curves represent the theoretical predictions for E_t given by Eqs. (13) and (14), respectively, with $C_1=0.017$ and $C_2=0.037$.

$$A_{t,\tau} \to A_t \quad \text{as } \tau \to t. \tag{9}$$

In Ref. [11], it was shown analytically and numerically that the error $|A_{t,\tau}(j,k)-A_t(j,k)|^2$ falls off as $T_{\rm cl}/\tau$ in a chaotic system, where $T_{\rm cl}$ is the time scale of classical correlations. This implies that for $\tau \gg T_{\rm cl}$ the approximate semiclassical correlator $A_{t,\tau}$ is closer to the exact semiclassical correlator than either is to the quantum dynamics:

$$|A_{t,\tau}-A_t| \ll |A_t-U_t|.$$

Thus

$$|A_{t,\tau}-U_t| \overset{\tau \gg T_{\rm cl}}{\to} |A_t-U_t| \tag{10}$$

allowing for an unambiguous determination of the error in the true semiclassical dynamics A_t at time t using $A_{t,\tau}$ and permitting a study of the breakdown of the semiclassical approximation at long times t where performing an exact sum over $O(e^{\lambda t})$ classical paths is impractical or impossible.

To confirm the convergence of the iterated propagator $A_{t,\tau}$ to the true long-time semiclassical propagator A_t for semiclassical dynamics in phase space, and specifically the convergence of the semiclassical error in accordance with Eq. (10), we first compute, as a function of time t, the average τ-semiclassical error defined as

$$\begin{aligned} E_{t,\tau} &= \| A_{t,\tau}-U_t\|^2 \\ &= \mathrm{Tr}[A_{t,\tau}-U_t]^\dagger[A_{t,\tau}-U_t] \\ &= \sum_{j,k} |A_{t,\tau}(j,k)-U_t(j,k)|^2. \end{aligned} \tag{11}$$

The results are shown in Fig. 1 for a chaotic kicked map defined by parameters $m_q=m_p=1$ and $K_q=K_p=1/2$, with semiclassical parameter $N=256$. We notice the relatively poor agreement between the iterated semiclassical calculation for $\tau=1$ and similar calculations for larger quantization times τ. We also note that using the iterated propagator with short quantization time τ overestimates the true size of the semiclassical error. At the same time, we observe rapid convergence of $E_{t,\tau}$ as $\tau \gg 1$, with the $\tau=5$ and $\tau=6$ curves lying almost on top of one another. Thus the τ-semiclassical error $E_{t,\tau}$ appears to be rapidly approaching the true semiclassical error

$$E_t = \sum_{j,k} |A_t(j,k)-U_t(j,k)|^2. \tag{12}$$

We are now ready to investigate the semiclassical error E_t as a function of time t and semiclassical parameter N. For a chaotic system, we may assume that the errors associated with the semiclassical approximation add incoherently as long as the times at which the errors occur are separated by at least the classical time scale $T_{\rm cl}$ [11]. Since the squared error in the semiclassical approximation over one time step is $E_1=O(h^2)=O(1/N^2)$, we obtain

$$E_t = C_1 h^2 t = hC_1\left(\frac{t}{N}\right), \tag{13}$$

where $C_1 \sim T_{\rm cl}$ is a system-dependent constant and we take $t=1$ to correspond to one period of the kicked map. The linear growth of the error predicted by Eq. (13) breaks down at times comparable to the Heisenberg time, where we must include an additional error term that is diagonal in the eigenbasis of the true quantum propagator U_1 [11]. The error associated with diagonal matrix elements adds coherently, leading to quadratic growth of the cumulative error in time. However, the fraction of diagonal matrix elements scales as $h=1/N$. Equation (13) must therefore be modified to read

$$E_t = C_1 h^2 t + C_2 h^3 t^2 = h\left[C_1\left(\frac{t}{N}\right) + C_2\left(\frac{t}{N}\right)^2\right]. \tag{14}$$

The data in Fig. 1 for $\tau \geqslant 4$ show good agreement with the prediction of Eq. (14), which is indicated by the upper solid curve. The linear growth indicated by Eq. (13), shown as the lower solid line, is valid for times t short compared with the Heisenberg time N.

In Fig. 2, we confirm the behavior predicted by Eqs. (13) and (14) as we vary the semiclassical parameter $N=1/h$. In this figure, the error $E_{\tau,t}$ has been scaled by a factor of N to make the curves at different values of N approximately coincide and to emphasize that the error at a fixed fraction of the Heisenberg time is falling off as $h \sim 1/N$ in the semiclassical limit $h \to 0$.

Specifically, we may ask about the size of the semiclassical error at the Heisenberg time itself, i.e., at $t/N=1$, which corresponds to the right edge of the graph in Figs.1 and 2. The scaling of the error at the Heisenberg time determines the feasibility of semiclassically computing individual eigenstates and eigenvalues in the limit of small $\hbar_{\rm eff}$, corresponding physically to the high-energy limit $E \gg E_{\rm gs}$. Based on Eq. (14), we predict the error at the Heisenberg time to be proportional to h:

$$E_{t=N} = h[C_1 + C_2]. \tag{15}$$

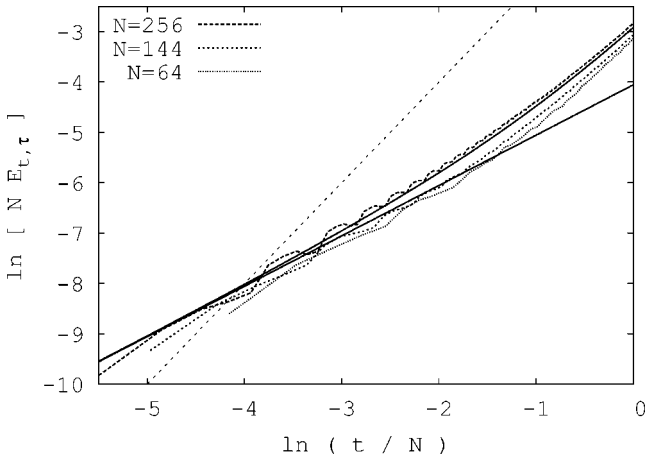

FIG. 2. The mean squared τ-semiclassical error $E_{t,\tau}$ for a chaotic system is plotted as a function of t/N for $\tau=5\gg1$ and several values of the semiclassical parameter $N=1/h=64$, 128, 256. The classical system parameters are the same as in the previous figure. The lower and upper solid curves represent the theoretical predictions of Eqs. (13) and (14), respectively. The dotted line indicates the predicted growth of the error for a system with *regular* dynamics, $E_t\sim t^2$ (see Sec. III B), and is shown to emphasize the qualitatively different behavior.

This prediction is tested in Fig. 3, where the black squares represent the numerical data and the corresponding solid line is a best fit to a power-law form, $E_{t=N}=ah^{\beta}=aN^{-\beta}$, with $\beta\approx0.8$. This is to be compared with the asymptotic prediction $\beta=1$ for $h\to0$. The falloff in the error with N shows that individual eigenstates and eigenvalues may be determined with ever improving accuracy as $N\to\infty$. As we will find in the following section, this is in contrast with the situation for systems with regular classical dynamics (see also the white squares in Fig. 3).

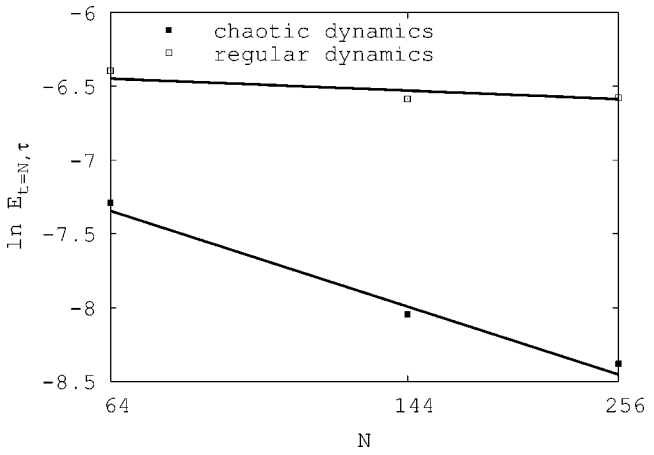

FIG. 3. The semiclassical error at the Heisenberg time, $E_{t=N,\tau}$ is plotted for $\tau=5\gg1$, and for three values of the semiclassical parameter $N=1/h$. Black squares correspond to the chaotic system of the previous two figures, while white squares correspond to the regular system of Sec. III B. The straight lines are fits to the power-law form $E_{t=N}=\alpha N^{-\beta}$, with the best fit giving $\beta_{\text{chaotic}}=0.8$ and $\beta_{\text{regular}}=0.1$, to be compared with the theoretical predictions $\beta_{\text{chaotic}}=1$ [Eq. (15)] and $\beta_{\text{regular}}=0$ [Eq. (21)].

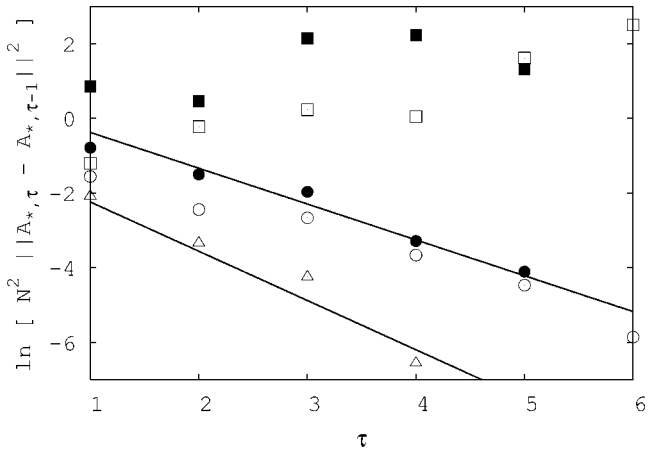

FIG. 4. The convergence of the finite-time approximation to the long-time one-step semiclassical propagator A_* is studied for several systems and different values of the semiclassical parameter $N=1/h$ [see Eq. (17)]. The circles represent data for the same system parameters that were used in the previous three figures, white and black circles corresponding to $N=64$ and $N=144$, respectively. White triangles represent data for $N=64$ with an alternative set of parameters: $m_q=2$, $m_p=1$, $K_q=K_p=1/2$ in Eq. (2), having a larger Lyapunov exponent. The solid lines for the two systems are the predictions of Eq. (18), with $\lambda=\cosh^{-1}(3/2)=0.96$ and $\lambda=\cosh^{-1}(2)=1.32$, respectively. The white and black squares ($N=64$ and $N=256$, respectively) represent data for the regular dynamics discussed in Sec. III B, where no convergence with τ is predicted or observed.

The semiclassical spectrum and semiclassical eigenstates can be obtained in principle by computing the semiclassical propagator A_t for long times and transforming into the energy domain. However, since the semiclassical propagator A_t at long times becomes approximately multiplicative [11],

$$A(t+1)\approx A_*A(t), \tag{16}$$

for some constant matrix A_*, it is much more convenient to diagonalize A_* directly to obtain the semiclassical eigenvalues and wave functions. We emphasize that A_* is neither the quantum evolution matrix U_1 nor the semiclassical evolution matrix A_1 for one time step, but is instead the effective one-step semiclassical propagator that describes semiclassical evolution at long times, and thus the stationary behavior of the semiclassical dynamics [11]. In practice, we may obtain $A_\star$ as the limit

$$A_*=\lim_{\tau\to\infty}A_{*,\tau}=\lim_{\tau\to\infty}A(\tau+1)[A(\tau)]^{-1}. \tag{17}$$

As discussed in Ref. [11], the convergence $A_{*,\tau}\to A_*$ is exponentially fast in τ, at least for the position space semiclassical propagator:

$$||A_{*,\tau}-A_*||^2\sim h^2e^{-\lambda\tau}. \tag{18}$$

In Fig. 4, we verify this convergence in the case of the phase space semiclassical propagator for two different values of $N=1/h$ (white and black circles). The rate of convergence λ is consistent with the classical value of the Lyapunov exponent, and is independent of $\hbar$. The white triangles correspond

to an example with a larger Lyapunov exponent [$m_q=2$, $m_p=1$, $K_q=K_p=1/2$ in Eq. (2)], where the convergence with τ is correspondingly faster.

Exponentially fast convergence to A_* with τ implies that the semiclassical spectrum and semiclassical wave functions can be obtained with very high accuracy using semiclassical dynamics for $t>1$ but still short compared to the Heisenberg time $t=N$ or even the log time T_{mix}. In other words, all the information needed to calculate long-time or stationary semiclassical properties is already contained in the short-time classical behavior, well before interference effects become relevant.

The stationary semiclassical spectrum and wave functions can now be compared with their quantum analogs. From the linear scaling with h of the error in the time evolution at the Heisenberg time, Eq. (15), which has been tested above in Fig. 3, we can deduce that the mean squared error in the eigenvalues must also scale linearly with h, ignoring a possible overall shift in the spectrum [12] which is absent in the present system due to symmetry. Thus

$$F=\frac{1}{N}\sum_{i=1}^{N}\frac{(\epsilon_{i,\mathrm{SC}}-\epsilon_i)^2}{\Delta^2}\sim h=\frac{1}{N}, \tag{19}$$

where the ϵ_i and $\epsilon_{i,\mathrm{SC}}$ are the quantum and semiclassical eigenvalues, and Δ is the mean level spacing. In practice, this improvement in the semiclassical approximation for individual eigenvalues as $h\to 0$ is difficult to measure due to numerical errors. For example, for the same chaotic system discussed previously ($m_q=m_p=1$, $K_q=K_p=1/2$), F is already 1.3×10^{-5} for $N=36$.

B. Regular dynamics

We may easily change parameters in Eq. (2) to obtain fully or almost fully stable classical dynamics and then repeat the semiclassical calculations and analysis of Sec. III A. We choose $m_p=1$, $m_q=-1$, $K_p=K_q=0.1$. The small nonlinearity parameters K_p and K_q have been selected to reduce the semiclassical error in the short-time propagator; as we will see below, the semiclassical error grows much faster with time here than in the chaotic case.

In a system with regular dynamics, a typical classical trajectory repeatedly visits the same regions of phase space, and errors in the semiclassical approximation are expected to add coherently [12]. Thus, in contrast with the chaotic case, the squared difference between the time evolution matrix for quantum dynamics and its semiclassical counterpart is expected to grow quadratically with time:

$$E_t=Ch^2t^2=C\left(\frac{t}{N}\right)^2, \tag{20}$$

where C is a classical constant that depends on the nonlinearity of the system, as well as on the typical number of kicks needed for a typical classical trajectory to return to the vicinity of its starting point. This quadratic growth of the error, even at times short compared to the Heisenberg time N, is to be contrasted with the result of Eq. (14) for a fully chaotic system. The prediction of Eq. (20) is tested in Fig. 5,

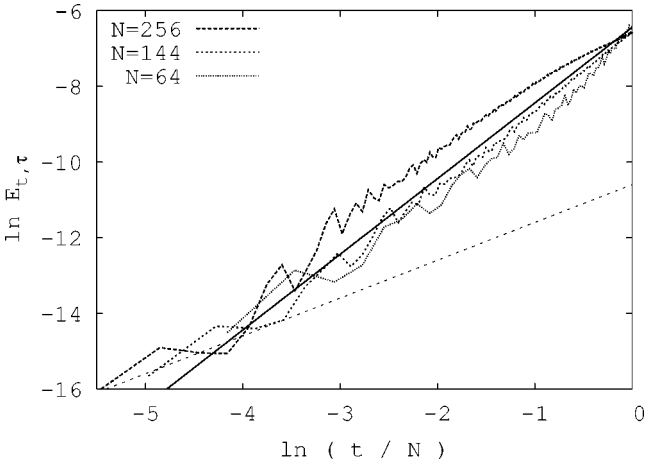

FIG. 5. The mean squared τ-semiclassical error $E_{t,\tau}$ for a system with regular dynamics, is plotted as a function of t/N for $\tau=5\gg 1$ and several values of the semiclassical parameter $N=1/h=64,128,256$. The classical system parameters are $m_p=1$; $m_q=-1$; $K_q=K_p=0.1$. The solid curve represents the theoretical prediction of Eq. (20), with $C=0.0016$. The dotted line corresponds to linear growth of the error with time, $E_t\sim t$, applicable to the chaotic case only [see Eq. (13) and Fig. 2], and is shown to emphasize the very different scaling behavior in the case of regular dynamics.

where the quadratic growth is confirmed as well as the predicted scaling with the semiclassical parameter $N=1/h$. Furthermore, the growth of the semiclassical error with time is completely different in the regular and chaotic case, as can be seen from the dotted lines in Figs. 2 and 5.

For a regular system at the Heisenberg time $t=N$, we obtain an $\hbar_{\mathrm{eff}}$-independent semiclassical error

$$E_{t=N}=C, \tag{21}$$

to be contrasted with the diminishing semiclassical error at the Heisenberg time in the $\hbar_{\mathrm{eff}}\to 0$ limit for a chaotic system, as indicated by Eq. (15). The Heisenberg-time error for our regular system is plotted for several values of N in Fig. 3. We note that the Heisenberg-time semiclassical error is larger for the regular system as compared with a chaotic system at the same value of N, despite the fact that the one-step semiclassical error is larger in the chaotic case.

The $O(\hbar^0)$ error in the semiclassical evolution at the Heisenberg time, as indicated by Eq. (21), suggests that semiclassical eigenvalues and wave functions, if they exist, do not approach the corresponding quantum eigenvalues and wave functions in the $\hbar_{\mathrm{eff}}\to 0$ limit. Instead, for a two-dimensional system with regular classical dynamics, the semiclassical error in the eigenvalues is proportional to the mean level spacing, implying that even the order of eigenvalues in the spectrum cannot be unambiguously determined using semiclassical methods.

The problem, however, is more serious still, as the semiclassical dynamics for a regular system does not in general approach a stationary behavior at long times. We recall that for a chaotic system, the dynamics at long times approaches multiplication by a constant matrix A_*, whose eigenvalues and wave functions determine the stationary properties of the

system. In contrast, for a regular system, the convergence of Eq. (17) does not hold, since the Lyapunov exponent vanishes. This lack of convergence is observed in the squares plotted in Fig. 4, where it is seen that successive approximations to A_* differ from one another at $O(1/N^2)=O(\hbar_{\text{eff}}^2)$. In other words, the eigenvalues of the matrix defining semiclassical evolution from time t to $t+1$ and the eigenvalues of the matrix defining semiclassical evolution from $t+1$ to $t+2$ differ from one another on the scale of a mean level spacing, so no unique semiclassical spectrum can be defined that describes the long-time semiclassical behavior.

We note that a system with regular dynamics may be separable, in which case one may have a special set of coordinates for which semiclassical dynamics is exact (just as semiclassics may be exact for special chaotic systems such as the cat maps). The above results apply to the general situation where separability may not hold, e.g., a pseudointegrable system or a generic polygonal billiard, and also to the separable case when the quantization is done in a set of coordinates other than the ones for which the equations of motion separate. Assuming the semiclassics is not exact, and independent of the initial size of the semiclassical error, the semiclassical accuracy will progressively improve in the $\hbar_{\text{eff}}\to 0$ or high-energy limit as long as the Lyapunov exponent λ is nonzero, until eventually individual eigenvalues and wave functions become semiclassically resolvable. In the case of zero Lyapunov exponent, this improvement does not occur.

C. Mixed dynamics

Generic two-dimensional systems are neither fully regular nor fully chaotic, and it is therefore of interest to study the issue of semiclassical-quantum correspondence in the general regime of "soft chaos." A mixed classical phase space can be obtained using parameters $m_q=K_p=0$, $m_p=K_q=1$ in Eq. (2); for this system approximately 48% of phase space is associated with the chaotic sea and the remainder consists of stable islands. Based on our discussion in Secs. III A and III B on the very different behavior of semiclassical accuracy in chaotic and regular systems, respectively, it is natural to ask whether semiclassical accuracy may vary with initial conditions in the case of a mixed phase space.

We define a local version of the mean squared eigenvalue error introduced in Eq. (19):

$$F_{\phi_k}=\sum_{i=1}^{N}|\langle\psi_i|\phi_k\rangle|^2\frac{(\epsilon_{i,\text{SC}}-\epsilon_i)^2}{\Delta^2}\sim h=\frac{1}{N}, \tag{22}$$

where ϕ_k is one of the Gaussian wave packets introduced in Sec. II, ψ_i and ϵ_i are the eigenstates and eigenvalues of the quantum dynamics, and $\epsilon_{i,\text{SC}}$ are the semiclassically obtained counterparts to ϵ_i. In other words, F_{ϕ_k} measures the error in the semiclassical eigenvalues, weighing each eigenvalue error by the overlap of the corresponding eigenstate with ϕ_k. A contour plot of F_{ϕ_k} versus phase space coordinates q_k, p_k is shown in Fig. 6(a), for $N=1/h=256$.

We see that the semiclassical error is peaked in the major stable regions of phase space, particularly in the large stable island surrounding the $q=p=0$ stable fixed point, and to a somewhat lesser extent in the islands associated with the period-2 orbit at $p=1/2$. In contrast, F_{ϕ_k} remains low in the region of the chaotic sea, for example, in the vicinity of the unstable orbit at $q=1/2$, $p=0$. The contour plot in Fig. 6(b) shows the fraction of each wave packet ϕ_k consisting of stable trajectories, and the similarity between the main features in the two parts of the figure strongly suggests a correspondence between semiclassical accuracy and classical phase space structure.

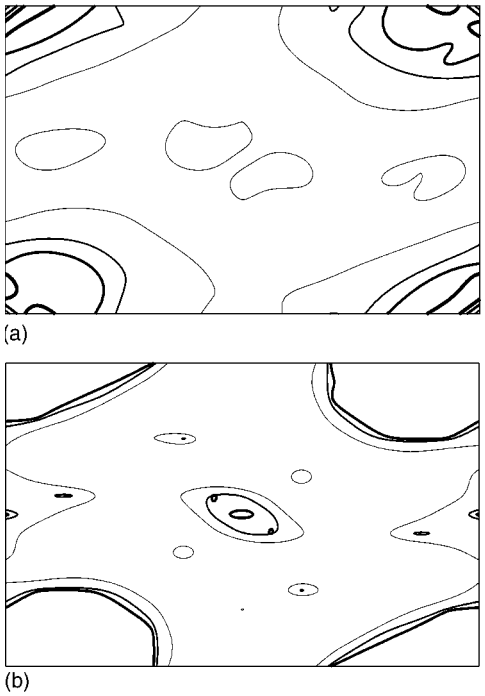

FIG. 6. (a) The weighted semiclassical eigenvalue error F_{ϕ_k} is plotted as a function of phase space location (q_k,p_k) for semiclassical parameter $N=256$. The contour curves correspond to $F=0.001$, 0.003, 0.005, 0.007 (the thickest curve indicates the largest error). The semiclassical eigenvalues are obtained by diagonalizing $A_{*,0}$ in Eq. (17). (b) For each wave packet ϕ_k used in (a), the fraction of stable trajectories for that wave packet is calculated classically and again plotted as a function of wave packet location. The contour curves correspond to stable fractions of 0.6, 0.9, 0.975 (the thickest curve corresponding to the most stable region).

The total semiclassical error for a mixed system is of course dominated by the error associated with the stable regions, and scales in the same way as the error for a regular system in Sec. III B.

IV. SUMMARY

Phase-space semiclassical propagation allows us to make direct comparison of semiclassical validity in chaotic and stable classical systems. Using the same semiclassical approximation in both cases results in a semiclassical error that scales with $\hbar$ in the same way at short times. However, the growth of the error with time is very different in the two situations. In the regular case, the error grows coherently because each trajectory repeatedly visits the same regions of

space phase; the mean squared error therefore grows quadratically with time. In the chaotic case, this coherence effect does not occur at times short compared with the Heisenberg time, resulting in a linear growth of the mean squared error.

At the Heisenberg time itself, the mean squared error in the propagator matrix elements becomes $O(1)$ in the case of a classically stable dynamics, making it impossible in general to speak of well-defined semiclassical wave functions or eigenvalues, i.e., ones that are independent of the choice of semiclassical coordinates. For a given choice of coordinates, semiclassical quantization generically will produce eigenvalues differing by the order of a mean level spacing from their quantum counterparts. Different semiclassical quantizations of a regular system will produce spectra differing from each other at the same order, making it impossible to uniquely determine even the order of eigenvalues in the spectrum via semiclassical methods (unless a particularly favorable set of coordinates can be chosen where semiclassics happens to be exact, e.g., for a separable dynamics).

In contrast, semiclassical dynamics at the Heisenberg time for a classically chaotic system becomes increasingly accurate as the system energy is increased. In the energy domain, the semiclassical error becomes a progressively smaller fraction of a mean level spacing, so the spectrum can be semiclassically determined with arbitrarily high accuracy when very highly excited states are considered. The convergence of semiclassical to quantum behavior for chaotic system is expected to be independent of the particular semiclassical method chosen (for example, it is independent of whether a position, momentum, or phase space semiclassics is used) as long as the methods have the same scaling with $\hbar$ at fixed time.

All calculations in the present paper were performed for time-dependent one-dimensional maps, whose scaling properties are equivalent to those of two-dimensional Hamiltonian systems. In $d=3$ dimensions, or in an interacting system, the Heisenberg time grows as a higher power of $\hbar^{-1}$ than in the two-dimensional single-particle case, resulting in a larger accumulated semiclassical error by the Heisenberg time for both chaotic and regular systems. For example, the same scaling argument that leads to Eq. (15) for $d=2$ chaotic systems predicts $O(1)$ semiclassical errors at the Heisenberg time for chaotic systems, independent of energy, i.e., eigenvalue errors that remain a constant fraction of a mean level spacing. In other words, the breakdown time of the semiclassical approximation will be proportional to the Heisenberg time in three dimensions, even when the dynamics is chaotic (and much shorter than the Heisenberg time for regular dynamics).

For $d \geqslant 4$, e.g., in the case of two interacting particles in two dimensions with no conserved quantities apart from total energy, the semiclassical approximation is expected to break down well before the Heisenberg time, even when the dynamics is fully chaotic. It would be interesting to investigate this behavior quantitatively for model systems, and also to ascertain how a higher-order semiclassical approximation may enable semiclassical methods to remain valid for interacting systems.

ACKNOWLEDGMENTS

This research was supported in part by the U.S. Department of Energy under Grant No. DE-FG03-00ER41132.

[1] S. Tomsovic and E. J. Heller, Phys. Rev. Lett. **67**, 664 (1991); M. A. Sepulveda, S. Tomsovic and E. J. Heller, *ibid.* **69**, 402 (1992).
[2] S. Tomsovic and E. J. Heller, Phys. Rev. E **47**, 282 (1993).
[3] P. A. Boasman, Nonlinearity **7**, 485 (1994).
[4] T. Prosen and M. Robnik, J. Phys. A **26**, L37 (1993).
[5] S. Rahav, O. Agam, and S. Fishman, J. Phys. A **32**, 7093 (1999).
[6] H. Primack and U. Smilansky, Phys. Rep. **327**, 1 (2000); J. Phys. A **31**, 6253 (1998); see also T. Prosen, Phys. Lett. A **233**, 323 (1997).
[7] J. Main, Phys. Rep. **316**, 233 (1999); K. Weibert, J. Main, and G. Wunner, Phys. Lett. A **289**, 329 (2001).
[8] P. Cvitanovic and B. Eckhardt, Phys. Rev. Lett. **63**, 823 (1989).
[9] J. Main, G. Wunner, E. Atilgan, H. S. Taylor, and P. A. Dando, Phys. Lett. A **205**, 176 (2002).
[10] E. G. Vergini, J. Phys. A **33**, 4709 (2000); E. G. Vergini and G. G. Carlo, *ibid.* **33**, 4717 (2000).
[11] L. Kaplan, Phys. Rev. E **58**, 2983 (1998).
[12] L. Kaplan, New J. Phys. **4**, 90 (2002).
[13] T. Prosen and M. Znidaric, J. Phys. A **35**, 1455 (2002); T. Prosen and T. H. Seligman, *ibid.* **35**, 4707 (2002).
[14] M. Gutzwiller, J. Math. Phys. **12**, 343 (1971).
[15] S. Fishman, D. R. Grempel, and R. E. Prange, Phys. Rev. Lett. **49**, 509 (1984); A. Altland and M. R. Zirnbauer, *ibid.* **77**, 4536 (1996).
[16] E. J. Heller, J. Chem. Phys. **62**, 1544 (1975).
[17] M. F. Herman and E. Kluk, Chem. Phys. **91**, 27 (1984).
[18] R. G. Littlejohn, Phys. Rep. **138**, 193 (1986); D. Huber, E. J. Heller, and R. G. Littlejohn, J. Chem. Phys. **89**, 2003 (1988).
[19] W. H. Miller and T. F. George, J. Chem. Phys. **56**, 5668 (1972).
[20] F.-M. Dittes, E. Doron, and U. Smilansky, Phys. Rev. E **49**, R963 (1994); L. Kaplan and E. J. Heller, Phys. Rev. Lett. **76**, 1453 (1996).
[21] A. K. Pattanayak and W. C. Schieve, Phys. Rev. E **50**, 3601 (1994).
[22] L. Kaplan, Phys. Rev. Lett. **81**, 3371 (1998).
[23] G. Tanner, P. Scherer, E. B. Bogomolny, B. Eckhardt, and D. Wintgen, Phys. Rev. Lett. **67**, 2410 (1991).
[24] E. B. Bogomolny, Comments At. Mol. Phys. **25**, 67 (1990).